Redox Biology 20 (2019) 261–274

Contents lists available at ScienceDirect

Redox Biology

journal homepage: www.elsevier.com/locate/redox

Research Paper

Mst1 deletion attenuates renal ischaemia-reperfusion injury: The role of microtubule cytoskeleton dynamics, mitochondrial fission and the GSK3β-p53 signalling pathway

Hongyan Li[a,*,1], Jianxun Feng[b,1], Yunfang Zhang[a], Junxia Feng[a], Qi Wang[a], Shili Zhao[a], Ping Meng[a], Jingchun Li[a]

[a] Department of Nephrology, Huadu District People's Hospital of Guangzhou, Southern Medical University, Guangzhou 510800, China
[b] Department of Nephorology, Xuhui DIstrict Centeral Hospital of Shanghai, Shanghai 20031, China

ARTICLE INFO

Keywords:
Renal ischaemia-reperfusion injury
Mitochondrial fission
F-actin
Drp1
GSK3β-p53 signalling pathway

ABSTRACT

Despite extensive research that has been carried out over the past three decades in the field of renal ischaemia-reperfusion (I/R) injury, the pathogenic role of mitochondrial fission in renal I/R injury is poorly understood. The aim of our study is to investigate the molecular mechanism by which mammalian STE20-like kinase 1 (Mst1) participates in renal I/R injury through modifying mitochondrial fission, microtubule cytoskeleton dynamics, and the GSK3β-p53 signalling pathway. Our data demonstrated that genetic ablation of Mst1 improved renal function, alleviated reperfusion-mediated tubular epithelial cell apoptosis, and attenuated the vulnerability of kidney to I/R injury. At the molecular level, Mst1 upregulation exacerbated mitochondrial damage, as evidenced by reduced mitochondrial potential, increased ROS generation, more cyt-c liberation from mitochondria into the cytoplasm, and an activated mitochondrial apoptotic pathway. Furthermore, we demonstrated that I/R-mediated mitochondrial damage resulted from mitochondrial fission, and the blockade of mitochondrial fission preserved mitochondrial homeostasis in the I/R setting. Functional studies have discovered that Mst1 regulated mitochondrial fission through two mechanisms: induction of Drp1 phosphorylation and enhancement of F-actin assembly. Activated Mst1 promoted Drp1 phosphorylation at Ser616, contributing to Drp1 translocation from the cytoplasm to the surface of the mitochondria. Additionally, Mst1 facilitated F-actin polymerization, contributing to mitochondrial contraction. Finally, we confirmed that Mst1 regulated Drp1 post-transcriptional modification and F-actin stabilization via the GSK3β-p53 signalling pathway. Inhibition of GSK3β-p53 signalling provided a survival advantage for the tubular epithelial cell in the context of renal I/R injury by repressing mitochondrial fission. Collectively, our study identified Mst1 as the primary pathogenesis for the development and progression of renal I/R injury via activation of fatal mitochondrial fission by modulating Drp1 phosphorylation, microtubule cytoskeleton dynamics, and the GSK3β-p53 signalling pathway.

1. Introduction

Renal ischaemia-reperfusion (I/R) injury primarily occurs upon the restoration of blood flow to the ischemic kidney in patients with infarction, sepsis or organ transplantation [1]. Renal I/R injury exacerbates tissue damage by inducing excessive oxidative stress, an uncontrolled inflammatory response and extensive renal tubular epithelial cell death [2]. Additionally, renal I/R injury is closely associated with acute kidney injury (AKI), contributing to rapid kidney dysfunction and high mortality rates [3]. Despite extensive research carried out over the past six decades in the field of renal I/R injury, the pathogenesis of I/R injury in the kidney is poorly understood [4]. Accordingly, a better understanding of the cellular pathophysiological response underlying kidney I/R injury will hopefully result in the design of more targeted therapies to prevent renal dysfunction.

Mitochondria, the cellular energy machinery, has been found to be associated with tissue I/R injury via pleiotropic effects [5,6]. In response to acute ischaemia attack, mitochondria are divided into several daughter mitochondria to ensure energy production [7]. However, at the stage of reperfusion, excessive mitochondrial fragmentation converts mitochondria from ATP providers that energise the cell to agents of cell death, akin to the dual effects of ROS in physical or pathological

* Corresponding author.
E-mail address: lihy0726@126.com (H. Li).
[1] The first authors equally contributed to this study.

https://doi.org/10.1016/j.redox.2018.10.012
Received 5 August 2018; Accepted 15 October 2018
Available online 19 October 2018

conditions on cell fate [8]. Most robust data concerning the relationship between mitochondrial fission and reperfusion-initiated cell injury have been provided by genetic loss- and gain-of-function studies. For example, inhibition of mitochondrial fission protects the mitochondrial redox balance, attenuates mitochondrial calcium overload [9], reduces the mPTP opening rate [10], sustains mitochondrial potential [11], reverses mitophagy activity [12], promotes mitochondrial ATP production [13], and prevents mitochondrial apoptosis activation [14]. However, the role of mitochondrial fission in renal I/R injury has not been appropriately investigated. At the molecular level, mitochondrial fission is executed via Drp1 translocation from the cytoplasm to the surface of the mitochondria [15]. Drp1 migration is highly regulated via post-transcriptional modifications, namely, phosphorylation. Phosphorylation of Drp1 at Ser616 promotes Drp1-related mitochondrial fission [16]. By contrast, phosphorylation of Drp1 at Ser637 combats Drp1 activation, thereby reducing mitochondrial fission [17]. Interestingly, no study is available to establish the regulatory effects of I/R injury on Drp1 phosphorylation in the kidney.

In addition to Drp1 phosphorylation, mitochondrial division is a process that is dependent on actin polymerization. Actin polymerization, which influences microtubule cytoskeleton dynamics, has been implicated as a force generator that mediates mitochondrial contraction [18]. Accumulative evidence has suggested the indispensable role of F-actin polymerization in mitochondrial fission [19]. For example, the induction of F-action depolymerization represses hyperglycaemia-mediated mitochondrial fission and sends a pro-survival signal to endothelial cells [16]. By comparison, activation of F-actin assembly promotes endometriotic apoptosis by augmenting mitochondrial fission [20]. Similarly, in cardiac I/R injury, F-actin disassembly is associated with mitochondrial fission inhibition and the increased resistance of cardiac microcirculation to I/R-mediated damage [6]. Starting from the necessary effect of F-actin polymerization in mitochondrial fission activation, it is worthwhile to explore the actions of microtubule cytoskeleton dynamics in renal I/R injury.

Mammalian STE20-like kinase 1 (Mst1), also known as serine/threonine-protein kinase 4, is the downstream effector of the Hippo signalling pathway. Several studies have suggested the causal relationship between Mst1 upregulation and cell death. Mst1 activation promotes hepatoma cell death via the PHLPPA-Akt signalling pathway [21]. Brain ischaemia-reperfusion injury and neuronal apoptosis are also related to Mst1 activation [22]. Mst1 also participates in atherosclerosis progression via autophagy inhibition and macrophage apoptosis [23]. Many researchers have attempted to demonstrate the promotive effects of Mst1 on acute cell death. However, no study has investigated the contribution of Mst1 to renal I/R injury. Moreover, Mst1 has been reported to be associated with mitochondrial damage in myocardial ischaemia reperfusion injury [24], pancreatic cancer cells [25], and spinal cord trauma [26]. This evidence supports the possibility that Mst1 can be considered the upstream regulator of mitochondrial homeostasis during acute cell stress. However, whether Mst1 can regulate mitochondrial fission via Drp1 post-transcriptionally and via microtubule cytoskeleton dynamics in the setting of renal I/R injury is incompletely understood. The aim of our study is to explore the detailed actions and mechanisms of Mst1 in renal I/R injury, with a focus on mitochondrial fission, Drp1 phosphorylation modification and microtubule cytoskeleton homeostasis.

2. Methods

2.1. Renal I/R injury model

The procedure of the I/R injury model was performed as previously described [27]. In short, I/R injury was achieved by unilateral clamping (micro aneurysm clamps) in one renal pedicle for 30 min under general inhalation anaesthesia (3% isoflurane and oxygen). Reperfusion was induced via removal of the clamps for approximately 4 h. Sham-operated mice underwent the same procedure except for clamping of the renal pedicles. Subsequently, the blood and reperfused kidneys were collected. To analyse renal function, the creatinine and blood urea nitrogen (BUN) levels were measured using the Cobas® C311 Auto-analyzer (Roche Diagnostics, Indianapolis, USA) according to the manufacturer's protocols. Urinary Kim-1 in mice was measured using a Luminex-based assay according to a previous study. Fg in urines was measured using commercially available species-specific Luminex-based assay kit from Millipore. ELISA kits obtained from Cusabio Technology (Wuhan, China) were applied to analyse the concentration of inflammation factors such as TNFα, MCP-1, and IL-6.

2.2. Histological evaluation

After creating the reperfusion model, the kidneys were isolated and then washed with PBS to remove the red blood cells. Next, the samples were fixed using 4% paraformaldehyde for 30 min at the room temperature. The sections were cut and stained with HE (haematoxylin and eosin) and Periodic Schiff-Methenamine (PASM) staining. The samples were then observed under an Olympus light microscope (Olympus, Tokyo, Japan). The histologic changes after tubular injury were evaluated semi-quantitatively by determining the percentage of tubules in the external medulla area where epithelial necrosis, loss of the brush border, cast formation, and/or tubular dilation were observed, according to a previous study. Images of the representative fields were captured [28].

2.3. Cell culture and treatment

The renal tubular epithelial cell line LLC-PK1, purchased from the American Type Culture Collection (ATCC® CL-101™) was cultured in DMEM medium (Gibco/Thermo Fisher, Waltham, MA, USA) supplemented with 10% FBS (Gibco/Thermo Fisher, Waltham, MA, USA) and 50 μg/mL penicillin and 50 μg/mL gentamicin in a humidified incubator at 37 °C and 5% CO_2. The growth medium was refreshed every 3 days. When the cells reached 70–80% confluence, they were treated with the hypoxia-reoxygenation (H/R) model in vitro. The H/R model was achieved via 30 min of hypoxia and 4 h of reoxygenation. Hypoxia preconditioning was performed using cells cultured in a tri-gas incubator with the N_2 concentration at 95% and CO_2 concentration at 5% for approximately 30 min. Next, reoxygenation injury was induced for 4 h in cells under normal culture conditions [29]. To induce mitochondrial fission, FCCP (5 μm; Selleck Chemicals, Houston, TX, USA) was applied for approximately 2 h to LLC-PK1 cells. To inhibit mitochondrial fission, mitochondrial division inhibitor 1 (Mdivi1; 10 mM; Sigma-Aldrich; Merck KGaA) was used for 12 h at 37 °C. SB216763 (20 μm; Selleck Chemicals, Houston, TX, USA) was used to inhibit GSK3β activity for 45 min.

2.4. Measurement of cell viability

The viability of the renal tubular epithelial cell line LLC-PK1 was monitored by the MTT assay and LDH release assay, according to the manufacturer's guidelines. Cells were plated at a density of 2×10^4 per well in 96-well plates. After H/R injury in vitro, 10 μl of MTT was added to each well, and the cells were incubated for 2 h at 37 °C. The number of viable cells was measured at 450 nm using a microplate reader (Bio-Rad 680). The results are presented as percentages of the values measured for untreated control cells. Independent experiments were performed in triplicate and repeated 3 times. The LDH release assay was performed according to the manufacturer's instructions [30].

Apoptosis in renal tissues and LLC-PK1 cell was identified via the terminal deoxynucleotidyl transferase-mediated dUTP nick-end labelling (TUNEL) assay using an in situ Cell Death Detection kit (Promega, Madison, WI, USA) according to the manufacturer's instructions. Five fields per section and three sections per kidney were examined in each

experimental group.

2.5. ATP detection

Cells were seeded in 6-well plates at 1×10^6 cells per well, and the cells were then incubated at 37 °C in 5% CO_2 until 80% confluent. The intracellular concentration of ATP was analysed using an ATP Assay Kit (Beyotime, China). To each well, 200 μl of lysate was added. The supernatant was collected after centrifugation for 5 min at 12,000*g* and 4 °C. The intracellular concentration of ATP was measured using a luminometer according to the protocol provided by Beyotime [31].

2.6. siRNA transfection and knockdown assay

Cells were seeded in 6-well clusters and then were incubated at 37 °C in 5% CO_2 until 80% confluent. Mst1 siRNA and Mfn2 siRNA were purchased from Santa Cruz, USA. siRNA transfection solution was prepared according to the directions provided by Santa Cruz to make a siRNA solution at a concentration of 400 nM. The cells were washed once with siRNA transfection medium (Santa Cruz, USA). Next, appropriate siRNA transfection medium and siRNA transfection solution were added to each well. The cells were then incubated for 6 h at 37 °C in 5% CO_2. The transfection mixture was then removed and replaced with normal growth medium, and then the cells were incubated for an additional 24 h. Western blotting was performed to observe the knockdown efficiency [32].

2.7. Immunofluorescence

After treatment, the cells were washed with cold PBS at room temperature. Next, the cells were fixed using 4% paraformaldehyde for 30 min at room temperature. To perform the immunofluorescence assay, the primary antibodies were incubated with the samples overnight at 4 °C. Subsequently, the samples were incubated with Alexa Fluor 488 donkey anti-rabbit secondary antibodies (1:1000; cat. no. A-21206; Invitrogen; Thermo Fisher Scientific, Inc.) for ~1 h at room temperature. DAPI was used to label the nuclei, and images were captured using an inverted microscope (magnification, ×40; BX51; Olympus Corporation, Tokyo, Japan) [33]. The primary antibodies used in the present study were as follows: cyt-c (1:500; Abcam; #ab90529), Tom 20 (mitochondrial marker, 1:1000, Abcam, #ab186735), F-actin (1:1000, Abcam, #ab205), G-actin (1:1000, Abcam, #ab200046), p53 (1:1000, Cell Signalling Technology, #9282), tubulin (1:1000, Cell Signalling Technology, #5335), p-Drp1-Ser616 (1:1000, Cell Signalling Technology, #3455), p-Drp1-Ser637 (1:1000, Cell Signalling Technology, #4867), p-GSK3β (1:1000, Cell Signalling Technology, #9322). Fluorescence intensity was calculated using Image-Pro Plus 6.0 software. Firstly, fluorescence pictures (red and green fluorescence) were converted to the grayscale pictures with the help of Image-Pro Plus 6.0 software. Then, red/green fluorescence intensities were separately recorded as the grayscale intensity. Subsequently, relative grayscale intensity was expressed as a ratio to that of control group.

2.8. ELISA

Cellular glutathione (GSH), glutathione peroxidase (GPx) and SOD were measured via ELISA according to the manufacturer's instructions. To analyse changes in caspase-3 and caspase-9, caspase-3/-9 activity kits (Beyotime Institute of Biotechnology) were used according to the manufacturer's protocol. To analyse caspase-3 activity, 5 μl DEVD-p-NA substrate (4 mM, 200 μM final concentration) was added to the samples for 2 h at 37 °C. To measure caspase-9 activity, 5 μl LEHD-p-NA substrate (4 mM, 200 μM final concentration) as added to the cell medium for 1 h at 37 °C. Subsequently, the wavelength at 400 nm was recorded via a microplate reader to reflect the caspase-3 and caspase-9 activities.

2.9. Measurement of reactive oxygen species (ROS) and mitochondrial membrane potential

To quantify the cellular ROS, flow cytometry was used. The cells were incubated with DHE on ice for 30 min, washed 3 times with PBS, and then isolated via enzyme digestion. The ROS level was quantified using a FACS flow cytometer (Becton Dickinson, USA). The mitochondrial membrane potential was measured using JC-1 staining. After H/R injury in vitro, the cells were washed with PBS three times and then were incubated with 5 mg/mL of JC-1 at 37 °C for 30 min. After washing with PBS three times, the images were visualized using a fluorescence microscope, and the red/green fluorescence was analysed using ImageJ software [13].

2.10. Western blotting

After treatment, the samples were collected and washed with ice-cold PBS and lysed with RIPA buffer, and the total protein concentration was measured using the BCA assay (Nanjing Keygen Biotech Co., Ltd., Nanjing, Jiangsu, China). A total of 50 μg of total protein for each sample was loaded into each well of a 15% SDS-PAGE gel, and then the proteins were separated by electrophoresis and transferred to PVDF membranes. After blocking in TBST with 10% non-fat milk for 2 h, the samples were incubated with primary antibodies overnight at 4 °C. After washing, the membranes were incubated with secondary antibody conjugated to horseradish peroxidase at 37 °C for 30 min. Finally, immunoreactive bands were visualized using a Super Signal West Pico kit according to the manufacturer's instructions [34]. The primary antibodies used in the present study were as follows: pro-caspase3 (1:1000, Abcam, #ab13847), cleaved caspase3 (1:1000, Abcam, #ab49822), Bcl2 (1:1000, Cell Signalling Technology, #3498), Bax (1:1000, Cell Signalling Technology, #2772), caspase9 (1:1000, Cell Signalling Technology, #9504), c-IAP (1:1000, Cell Signalling Technology, #4952), cyt-c (1:1000; Abcam; #ab90529), Drp1 (1:1000, Abcam, #ab56788), p-Drp1-Ser616 (1:1000, Cell Signalling Technology, #3455), p-Drp1-Ser637 (1:1000, Cell Signalling Technology, #4867), Opa1 (1:1000, Abcam, #ab42364), Mfn2 (1:1000, Abcam, #ab57602), Mff (1:1000, Cell Signalling Technology, #86668), p53 (1:1000, Cell Signalling Technology, #9282), Mst1 (1:1000, Cell Signalling Technology, #3682), F-actin (1:1000, Abcam, #ab205), G-actin (1:1000, Abcam, #ab200046), p-GSK3β (1:1000, Cell Signalling Technology, #9322), GSK3β (1:1000, Cell Signalling Technology, #5676), Mid49 (1:1000, Abcam, #ab101350), Mid51 (1:1000, Abcam, #ab89944). Band intensities were normalized to the respective internal standard signal intensity (GAPDH (1:1000, Cell Signaling Technology, #5174) and/or β-actin (1:1000, Cell Signalling Technology, #4970) using Quantity One Software (version 4.6.2; Bio-Rad Laboratories, Inc.). The relative expression of targeted proteins was normalized to GAPDH or β-actin.

2.11. Statistical analyses

All experiments were repeated at least 3 times for each group, and the data are presented as the means ± SEM. The data were analysed by ANOVA, followed by Fisher's least significant difference test, using SPSS software, version 13.0 (SPSS, Chicago, IL, USA).

3. Results

3.1. Increased Mst1 promotes renal I/R injury

First, renal I/R injury was performed in vivo by applying 30 min of ischaemia followed by 4 h of reperfusion. Next, Mst1 expression was monitored via qPCR and western blotting. Compared with the sham group, Mst1 expression was increased in the reperfused kidneys at both the transcriptional and translational levels (Fig. 1A-C). To verify

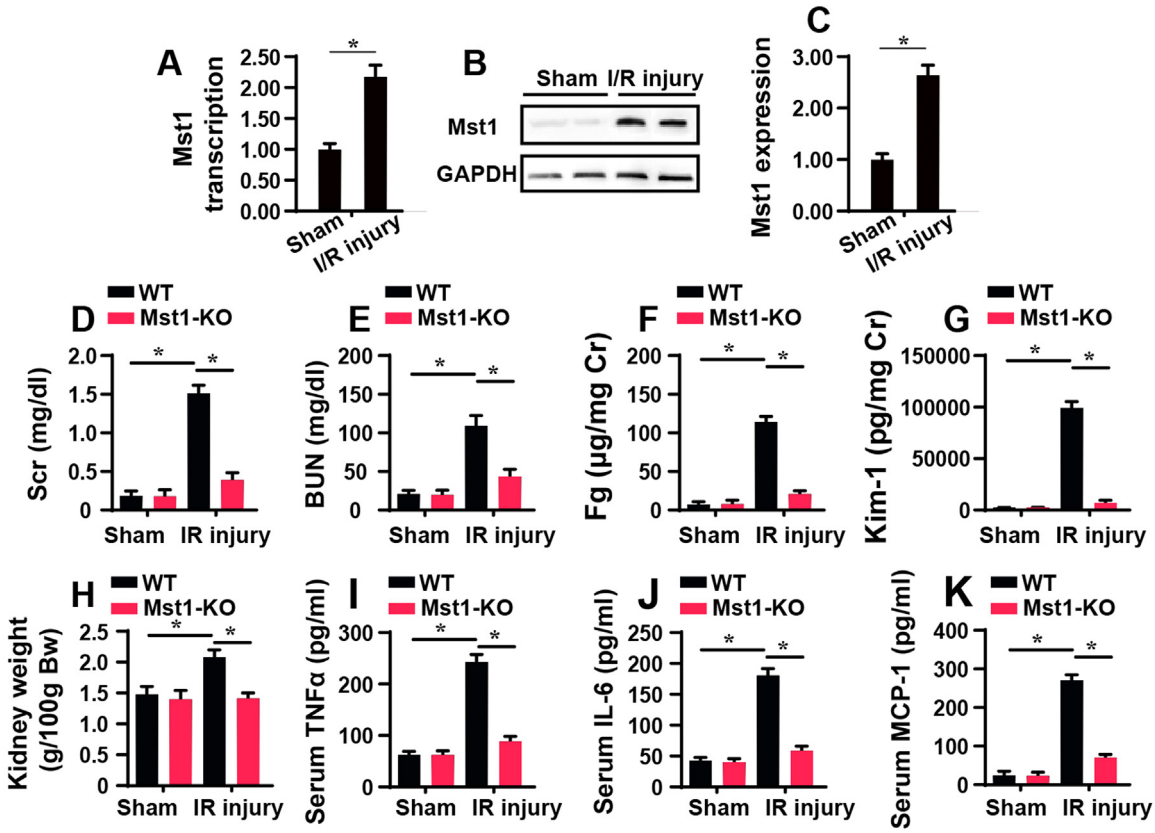

Fig. 1. Mst1 deletion reduces reperfusion-mediated renal damage. A. WT mice were subjected to IR injury. Then, the reperfused kidneys were isolated and the alteration of Mst1 was monitored via qPCR. **B-C.** Western blotting was performed to analyse the expression of Mst1 in response to renal I/R injury. **D-E.** The Scr and BUN was measured using ELISA. **F-G.** The kidney proximal tubular injury was evaluated via detecting the concentration of urinary Kim-1 and Fg. **H.** The alteration of kidney weight before and after I/R injury. **I-K.** ELISA was used to analyse the levels of inflammation factors after renal I/R injury. *P $<$ 0.05.

whether upregulated Mst1 was harmful to kidneys after I/R injury, Mst1-knockout (Mst1-KO) mice were used. Additionally, renal function was measured in mice that underwent I/R injury. Compared with the sham group, the levels of Scr and BUN were significantly increased in the mice treated with I/R injury and were downregulated in Mst1-KO mice (Fig. 1D-E). Moreover, kidney proximal tubular injury (measured via urinary levels of Kim-1 and Fg) was also enhanced in I/R-treated mice and was attenuated by Mst1 deletion (Fig. 1F-G). Moreover, the total kidney weight was increased in response to I/R injury and was reversed to near-normal levels with Mst1 deletion (Fig. 1H). This information indicated that Mst1 deletion reduced kidney damage in the context of renal I/R injury. Additionally, renal I/R injury elevated the concentrations of inflammatory factors such as TNFα, MCP1 and IL-6 (Fig. 1I-K), and these effects were negated by Mst1 deletion. Altogether, our data demonstrate that Mst1 is increased in response to renal I/R injury, and higher Mst1 expression is associated with kidney damage.

3.2. *Mst1 deletion sustains renal function after I/R injury*

The subsequent experiments were performed to observe the alterations of renal histology. As shown in Fig. 2A-E, compared with the sham group, I/R injury induced proximal tubular damage, as evidenced via HE staining and PASM staining. Interestingly, Mst1 deletion attenuated tubular damage compared with the kidneys of the sham-operated group (Fig. 2A-E). Additionally, the TUNEL assay was used to observe the cell apoptosis exerted by renal I/R injury. Compared with the sham group, the number of TUNEL-positive cells was increased to ~ 30% (Fig. 2F-G), whereas Mst1 deletion repressed the apoptotic index to ~ 10% (Fig. 2F-G). This finding was further supported by western blotting. As shown in Fig. 2H-N, I/R injury upregulated the expression of proteins related to cell apoptosis such as Bax, caspase-3 and caspse-9. However, the levels of anti-apoptotic proteins were unfortunately downregulated in response to I/R injury. Interestingly, Mst1 deletion could reverse the balance between anti- and pro-apoptotic factors (Fig. 2H-M).

3.3. *Mst1 deficiency attenuates reperfusion-mediated mitochondrial apoptosis*

Subsequently, the renal tubular epithelial cell line LLC-PK1 was used in vitro with a hypoxia and reoxygenation (H/R) stimulus to mimic animal I/R injury. To further provide more solid evidence of the role of Mst1 in reperfusion-mediated renal damage, siRNA against Mst1 was transfected into the LLC-PK1 cell line. Next, cell viability and apoptosis were evaluated via MTT assay and TUNEL staining, respectively. Compared with the control group, H/R injury significantly reduced cell viability (Fig. 3A) and increased the apoptotic ratio (Fig. 3B-C) of LLC-PK1 cells. Interestingly, H/R-mediated cell death was mostly repressed by Mst1 deletion. Mitochondrial damage has been acknowledged as a primary factor responsible for reperfusion-mediated renal injury. Accordingly, mitochondrial homeostasis was measured with or without Mst1 deletion in the setting of H/R injury. First, mitochondrial function was monitored via ATP production. Compared with the control group, H/R injury suppressed the concentration of cellular ATP (Fig. 3D), and this effect was nullified by Mst1 deletion. ATP production is primarily regulated by mitochondria, which convert the mitochondrial electric potential energy into chemical energy via the mitochondrial respiratory complex. Interestingly, the mitochondrial electric potential, as assessed by JC-1 staining, was decreased under H/R injury and was increased to near-normal levels with Mst1 deletion (Fig. 3E-F).

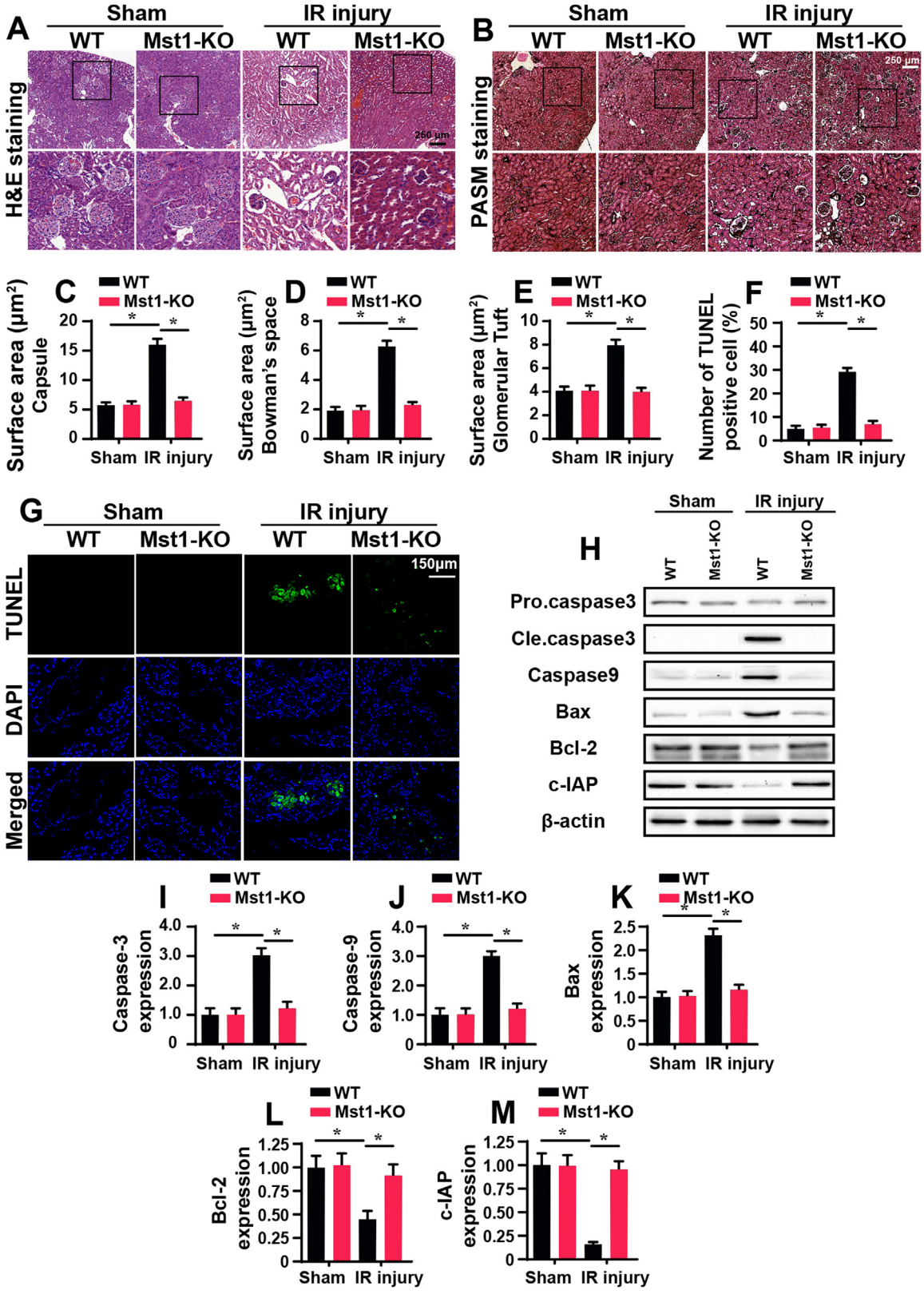

Fig. 2. Mst1 deficiency attenuates I/R-mediated cell death. A. HE staining was conducted to observe the IR-mediated renal damage. **B-E.** The histologic changes of tubular injury after renal IR damage was determined via PASM staining. **F-G.** The cell death was quantified via TUNEL assay and the number of TUNEL-positive cell was recorded. **H-M.** After renal I/R injury, the kidney tissues were collected and the proteins related to mitochondrial apoptosis were measured via western blotting. I/R increased the expression of pro-apoptotic proteins, and this effect was reversed by Mst1 deletion. *P < 0.05.

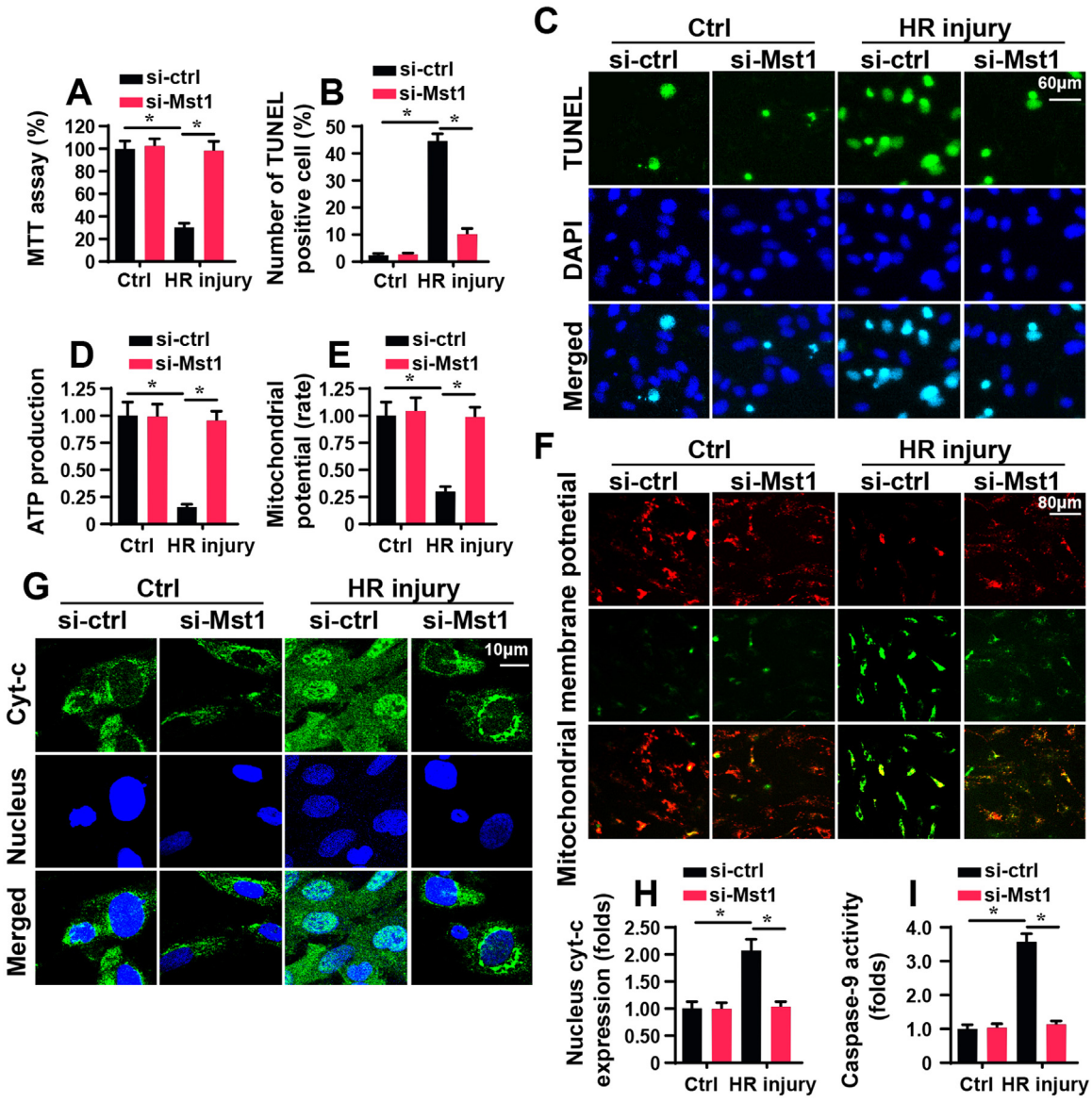

Fig. 3. Loss of Mst1 sustains mitochondrial homeostasis. A. In vitro, the renal tubular epithelial cell line LLC-PK1 was used with a hypoxia and reoxygenation (H/R) stimulus to mimic animal I/R injury. siRNA against Mst1 and control siRNA were transfected into cell in vitro. Then, MTT assay was performed to analyse the cellular viability. **B-C.** TUNEL assay was conducted to observe the cell death. The number of TUNEL-positive cell was increased in response to H/R injury and was reduced with Mst1 deletion. **D.** ATP production was measured to reflect the mitochondrial function. **E-F.** Mitochondrial potential was observed via JC-1 staining. The ratio of red to green fluorescence was recorded to quantify the mitochondrial potential (rate). **G-H.** Immunofluorescence assay for cyt-c. DAPI was used to tag the nucleus. H/R promoted cyt-c liberation into nucleus and this effect was reversed by Mst1 deletion. **I.** Mitochondrial apoptosis was assessed via analysing caspaase-9 activity. The relative caspase-9 activity was recorded as the ratio to control group. *P $<$ 0.05.

In response to mitochondrial potential reduction, mitochondria liberate the pro-apoptotic factors, such as cyt-c, into the cytoplasm/nucleus, opening the caspase-9-related mitochondrial apoptotic pathway [35]. The immunofluorescence assay in Fig. 3G-H demonstrates that H/R injury induced more cyt-c leakage into the cytoplasm/nucleus; this effect was mostly inhibited by Mst1 deletion in LLC-PK1 cells (Fig. 3G-H). Because of cyt-c liberation, the caspase-9 activity was increased in H/R-treated cells and was decreased in response to Mst1 deletion (Fig. 3I), suggesting that H/R-activated caspase-9-related mitochondrial apoptosis was repressed by Mst1 deletion. Taken together, the above data substantiated the sufficiency of pathogenically relevant degrees of reperfusion insult to induce renal damage, as well as the necessity of Mst1 for the H/R-initiated mitochondrial apoptosis in renal tubular epithelial cells.

3.4. Excessive mitochondrial fission accounts for Mst1-mediated mitochondrial apoptosis

To understand the mechanism by which Mst1 modulates mitochondrial apoptosis in the setting of renal I/R injury, we focused on mitochondrial fission, which was reported to be the early hallmark of mitochondrial damage in cerebral and cardiac I/R injury [7]. To identify mitochondrial fission, immunofluorescence assay for mitochondria was carried out. As shown in Fig. 4A, compared with the control group, H/R injury forced the mitochondria to divide into several fragmented mitochondria with shorter diameters, and this effect was negated by Mst1 deletion. To further quantify the mitochondrial fission, we measured the average length of mitochondria. The average length of normal mitochondria was ~8.1 μm (Fig. 4B). Interestingly, after H/R injury, the average length of mitochondria was decreased to

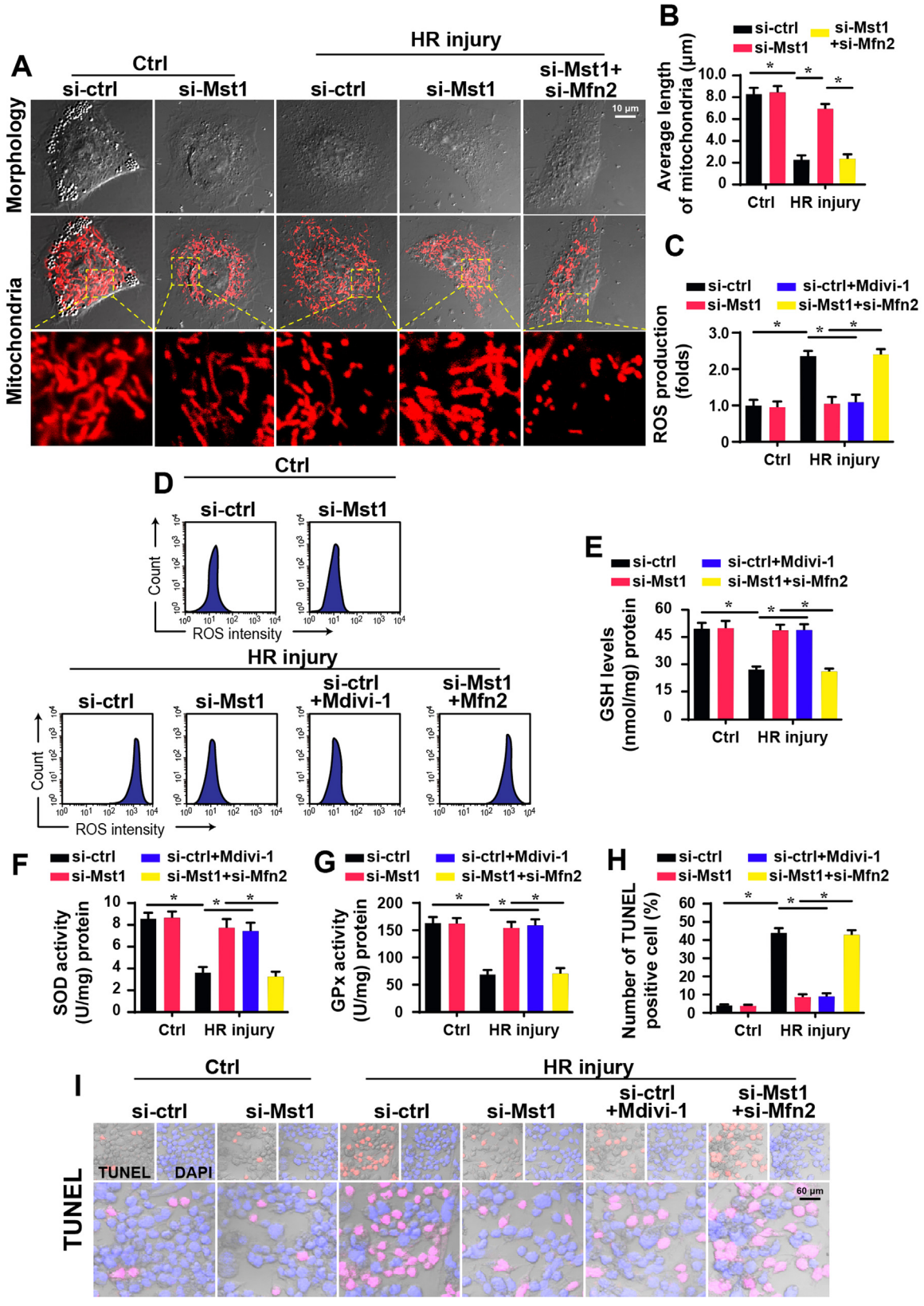

Fig. 4. H/R injury activates mitochondrial fission via Mst1. A. Mitochondrial fission was assessed via immunofluorescence using Tom-20 antibody. Mfn2 siRNA (si-Mfn2) was transfected into cell to re-activate mitochondrial fission. **B.** The average length of mitochondria was recorded, which was used to quantify the mitochondrial fission in response to H/R injury and Mst1 deletion. siRNA against Mst1 and control siRNA were transfected into cell in vitro**. C-D.** Cellular ROS generation was measured via DHE probe using flow cytometry. Mdivi1-1, the inhibitor of mitochondrial fission, was added into H/R-treated cell, which was used as the negative control group. Mfn2 siRNA (si-Mfn2) was administrated into Mst1-deleted cell, which was used to re-activate the mitochondrial fission. **E-G.** The concentrations of antioxidant were measured via ELISA. siRNA against Mst1 and control siRNA were transfected into cell. Mdivi1-1, the inhibitor of mitochondrial fission, was added into H/R-treated cell, which was used as the negative control group. Mfn2 siRNA (si-Mfn2) was administrated into Mst1-deleted cell, which was used to re-activate the mitochondrial fission. **H-I.** TUNEL assay was performed to observe the cell death in response to mitochondrial fission activation/inhibition.

~ 2.3 μm (Fig. 4B), and this effect was rescued by Mst1 deletion, which reversed the mitochondrial length to ~ 7.2 μm. This information indicated that H/R injury activated mitochondrial fission via Mst1. Subsequently, we questioned whether mitochondrial fission accounted for Mst1-mediated mitochondrial damage. To address this question, the mitochondrial fission inhibitor Mdivi-1 was added to the H/R-treated cells, which were used as the negative control group. Additionally, mitochondrial fission was re-activated via transfection of Mfn2 siRNA (si-Mfn2) in Mst1-deleted cells, which were used as the positive control group. Next, mitochondrial damage parameters were evaluated again. First, cellular ROS, as assessed via flow cytometry, was increased in response to H/R injury compared with that in the control group (Fig. 4C-D). However, Mst1 deletion repressed H/R-mediated ROS overproduction, similar to the results obtained with Mdivi-1 administration. Interestingly, reactivation of mitochondrial fission via si-Mfn2 transfection abrogated the inhibitory effect of Mst1 deletion on H/R-mediated oxidative stress (Fig. 4C-D). Because of the cellular redox imbalance, the concentration of antioxidant was decreased in H/R-treated cells and was reversed to near-normal levels with Mst1 deletion or Mdivi-1 treatment (Fig. 4E-G). Notably, activation of mitochondrial fission via si-Mfn2 transfection caused a drop again in the antioxidant content in Mst1-deleted cells (Fig. 4E-G). Besides, we also found that H/R-mediated cell death could be inhibited by Mst1 deletion and this effect was abrogated by Mdivi-1 treatment (Fig. 4H-I). Altogether, these data support the functional importance of mitochondrial fission in promoting Mst1-mediated renal mitochondrial damage in the context of kidney I/R injury.

3.5. Mst1 enhances reperfusion-mediated mitochondrial fission via Drp1 phosphorylation at Ser616

At the molecular level, mitochondrial fission was modulated by Drp1 phosphorylation [16]. Phosphorylated Drp1 was translocated from the cytoplasm to the surface of the mitochondria, forming a contractive ring around the mitochondria and then forcing the mitochondria divide into several fragments. Based on this information, we observed Drp1 phosphorylation using western blotting. As shown in Fig. 5A-C, compared with the control group, H/R injury promoted the phosphorylation of Drp1 at Ser616 but had no influence on the phosphorylation of Drp1 at Ser637. Interestingly, H/R-mediated Drp1 phosphorylation was reversed by Mst1 deletion (Fig. 5A-C). This information was further supported by immunofluorescence for phosphorylated Drp1. The fluorescence intensity of p-Drp1^{S616} was significantly increased in response to H/R injury and was decreased to near-normal levels with Mst1 deletion (Fig. 5D). However, no significant difference was observed with respect to the fluorescence intensity of p-Drp1^{S637} (Fig. 5D). This information indicated that Mst1-modified Drp1 phosphorylation was post-transcriptionally regulated by Drp1 phosphorylation at Ser616.

Because of Drp1 phosphorylation, mitochondrial fission factors such as Fis1, Mff, Mid49 and Mid51 were upregulated in response to Mst1 deletion (Fig. 5E-K); this effect was reversed by Mst1 deletion. Additionally, we observed other mitochondrial fusion factors such as Opa1 and Mfn2, which could be considered antagonists of mitochondrial fission. Interestingly, the Opa1 and Mfn2 expression levels were both downregulated by H/R injury and were reversed to near-normal levels after Mst1 deletion (Fig. 5E-K). Altogether, our data indicated that Mst1 modulated H/R-mediated mitochondrial fission via post-transcriptional modification of Drp1 at Ser616

3.6. Mst1 also regulates mitochondrial fission by promoting F-actin polymerization

In addition to Drp1 phosphorylation, F-actin polymerization was required for mitochondrial fission. In the present study, we found that F-actin expression was increased in H/R-treated cells compared with the control group (Fig. 6A-C). Notably, F-actin consists of G-actin, and the increase in F-actin was closely followed by a drop in G-actin (Fig. 6A-C), suggesting that H/R injury promoted G-actin assembly into F-actin. Interestingly, Mst1 deletion repressed F-actin and increased the content of G-actin in H/R-treated cells (Fig. 6A-C). Subsequently, this finding was further supported by immunofluorescence for F-actin. Compared with the control group, the F-actin florescence intensity was significantly increased in H/R-treated cells and was decreased to near-normal levels with Mst1 deletion (Fig. 6D-F). Notably, to investigate whether F-actin was specifically regulated by Mst1, we observed alterations in tubulin, another element of the cytoskeleton that plays no role in mitochondrial fission. Interestingly, neither H/R injury nor Mst1 deletion influenced tubulin expression compared with the baseline level (Fig. 6D-F), suggesting that Mst1 exclusively regulated F-actin in the context of renal I/R injury.

To provide more solid evidence for the role of Mst1-modified F-actin in mitochondrial fission, the F-actin stabilizer (Jasplakinolide; Jasp) was added to Mst1-deleted cells to repress Mst1 deletion-mediated F-actin depolymerization. Next, co-immunofluorescence for mitochondria and F-actin was performed. As shown in Fig. 6G, compared with the control group, H/R injury increased the fluorescence intensity of F-actin that was accompanied with a drop in the average length of mitochondria (Fig. 6H). Interestingly, Mst1 deletion repressed F-actin upregulation and inhibited H/R-mediated mitochondrial fission, and this effect was negated by Jasp treatment. These data indicated that F-actin polymerization was necessary for Mst1-mediated mitochondrial fission in the context of renal I/R injury. To then end, TUNEL assay was performed to confirm whether F-actin polymerization was also involved in fission-related cell death in the setting of H/R injury. As shown in Fig. 6I-J, H/R-mediated cell death could be inhibited by Mst1 deletion, and this effect was abrogated by Jasp treatment.

3.7. Mst1 regulates Drp1 phosphorylation and F-actin polymerization by activating the GSK3β-p53 axis

The following analysis was conducted to determine the mechanism by which Mst1 modulated Drp1 phosphorylation and F-actin polymerization in the H/R setting. A previous study reported the deleterious role played by GSK3β-p53 signalling in heart and liver reperfusion injury via modulation of mitochondrial homeostasis [36,37]. However, whether the GSK3β-p53 cascade was signalled by Mst1 and consequently regulated mitochondrial fission in renal I/R injury has not been demonstrated. Accordingly, GSK3β phosphorylation (its inactive status) and p53 upregulation were measured by western blotting. In the present study, we found that GSK3β phosphorylation was repressed by H/R injury (Fig. 7A-C), indicating the activation of GSK3β by H/R attack. Moreover, p53 expression was upregulated by H/R stimulus (Fig. 7A-C). Interestingly, Mst1 deletion augmented the GSK3β phosphorylation and repressed p53 expression under H/R stress (Fig. 7A-C). This finding was further supported by immunofluorescence for GSK3β phosphorylation and p53 (Fig. 7D-F). Altogether, our data indicated that Mst1 modulated the GSK3β-p53 signalling pathway in the setting of H/R injury. To validate whether the GSK3β-p53 axis is required for Mst1-mediated Drp1 phosphorylation and F-actin polymerization, the GSK3β inhibitor SB216763 was administered in H/R-challenged cells, which were used as the negative control group. Then, Drp1 phosphorylation and F-actin accumulation were observed via immunofluorescence. As shown in Fig. 7G-I, Mst1 deletion repressed H/R-mediated Drp1 phosphorylation and F-actin upregulation, similar to the results obtained by SB216763 treatment. To the end, to confirm whether GSK3β directly regulated mitochondrial fission, immunofluorescence assay was used. As shown in Fig. 7J-K, H/R-activated mitochondrial fission could be inhibited by Mst1 deletion and/or SB216763, suggesting that GSK3β inhibition directly attenuated H/R-mediated mitochondrial fission. Taken together, the GSK3β-p53 signalling pathway was, to some extent, involved in Mst1-mediated Drp1 phosphorylation and F-actin

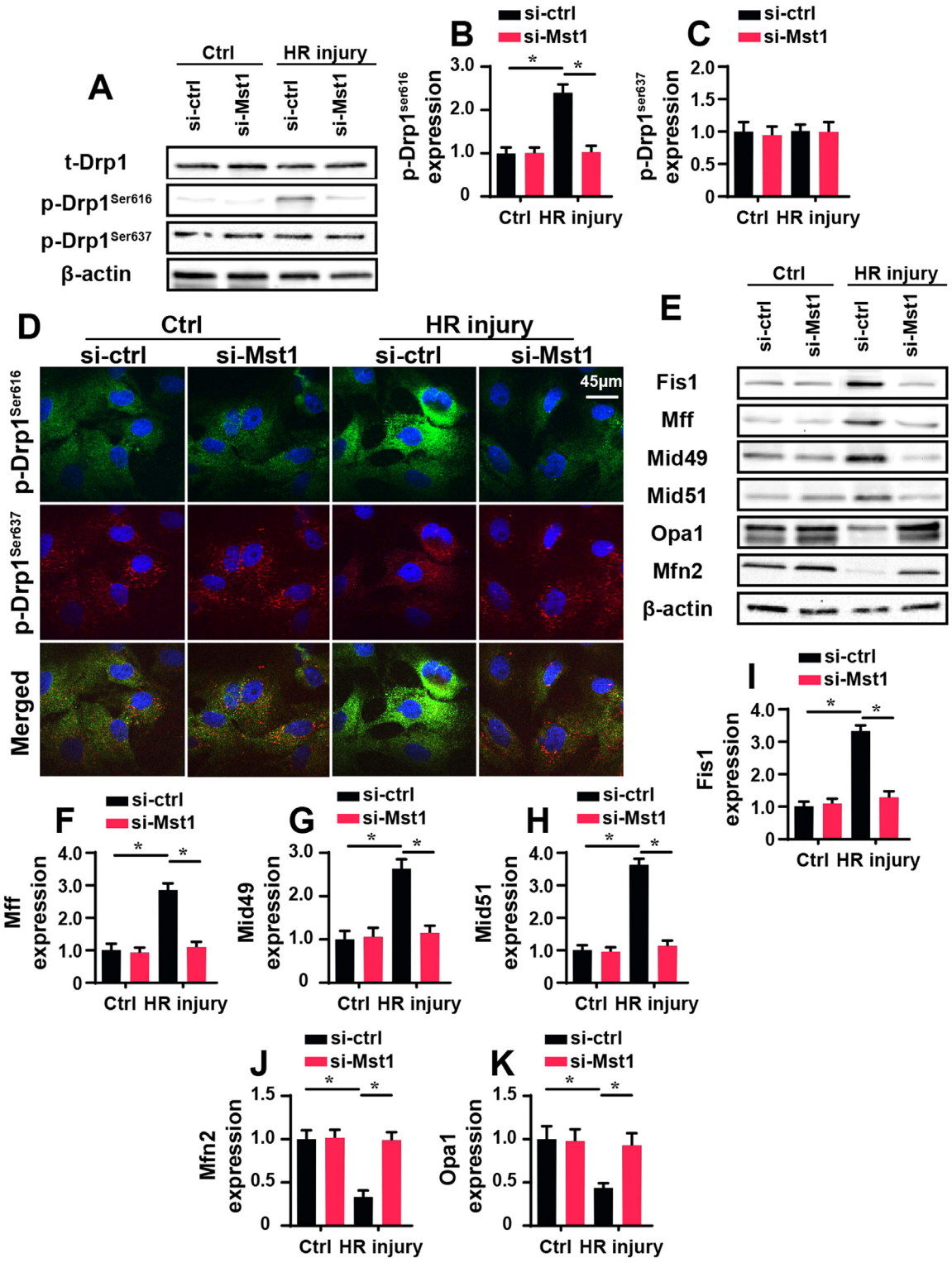

Fig. 5. Mst1 regulates mitochondrial fission via promoting Drp1 phosphorylation at Ser616 site. A-C. In vitro, the renal tubular epithelial cell line LLC-PK1 was used with a hypoxia and reoxygenation (H/R) stimulus to mimic animal I/R injury. siRNA against Mst1 and control siRNA were transfected into cell in vitro. Western blotting was performed to analyse the Drp1 phosphorylation. **D.** Immunofluorescence assay for Drp1 phosphorylation. **E-K.** After H/R injury, the protein was isolated and western blotting was performed to detect the protein expression related to mitochondrial fission. Besides, mitochondrial fusion-related factors such as Opa1 and Mfn2 were measured via western blotting. *P $<$ 0.05.

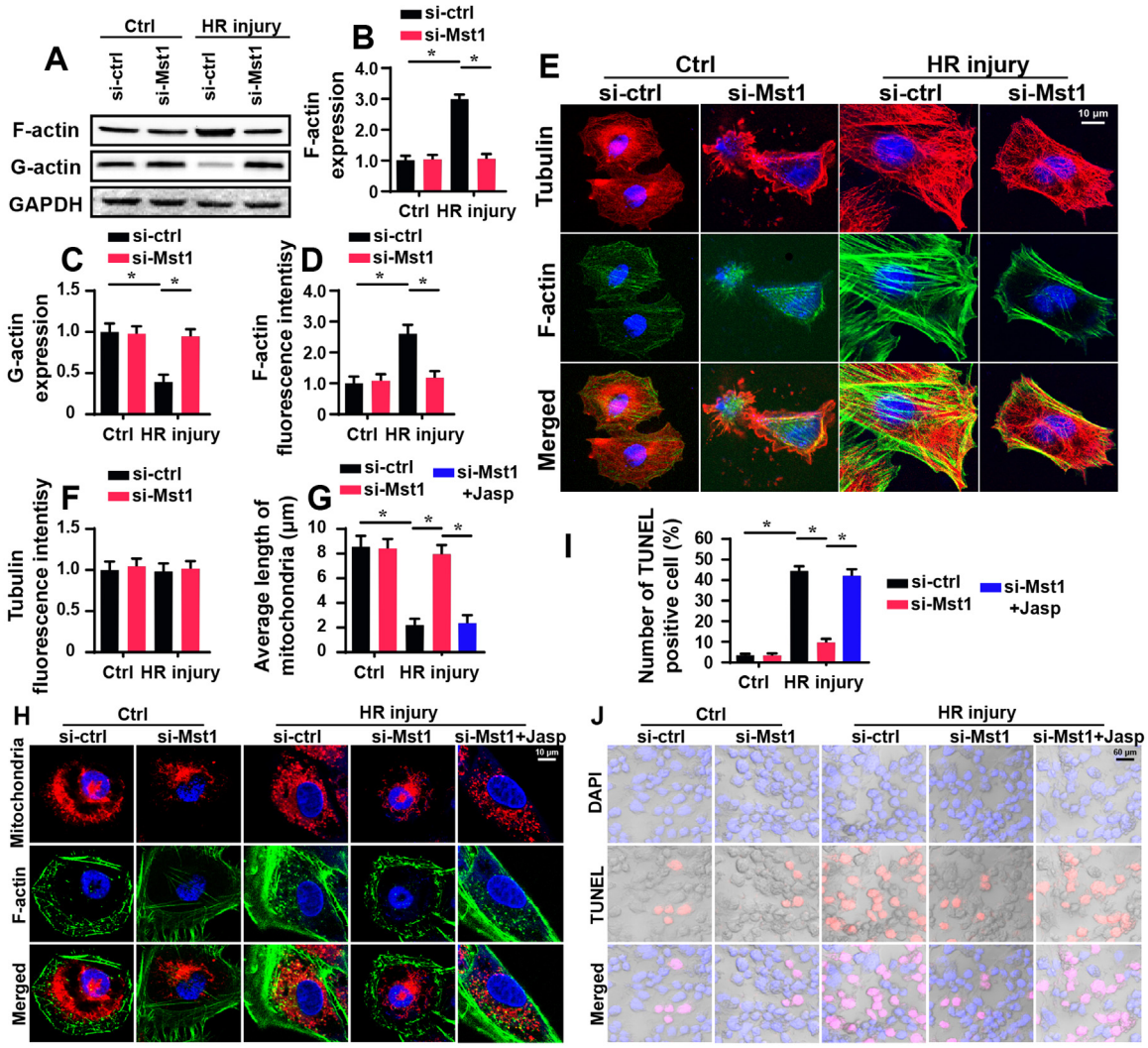

Fig. 6. Mst1-mediated F-actin accumulation contributed to mitochondrial fission under H/R injury. A-C. In vitro, the renal tubular epithelial cell line LLC-PK1 was used with a hypoxia and reoxygenation (H/R) stimulus to mimic animal I/R injury. siRNA against Mst1 and control siRNA were transfected into cell in vitro. Western blotting was performed to analyse the levels of F-actin and G-actin. **D-F.** immunofluorescence assay for F-actin polymerization. Tubulin was used as the control protein. **G-H.** F-actin stabilizer (Jasplakinolide; Jasp) was added in Mst1-deleted cell, which was used to reverse F-actin expression. Then, mitochondrial fission and F-actin expression were evaluated via immunofluorescence using Tom-20 and F-actin antibodies. The average length of mitochondria was measured. **I-J.** TUNEL assay was performed to observe the cell death in response to Jasp treatment. *P < 0.05.

recruitment in the setting of renal I/R injury.

3.8. The GSK3β-p53 axis is also involved in mitochondrial dysfunction and cell apoptosis

To this end, we explored whether the GSK3β-p53 axis was also implicated in mitochondrial dysfunction and renal tubular epithelial cell apoptosis. First, the LDH release assay was performed to analyse cell death. Compared with the control group, H/R injury elevated the content of LDH in the medium, and this effect was reversed by Mst1 deletion or treatment with SB216763 (Fig. 8A). Moreover, the MTT assay also demonstrated that the cell viability was decreased in response to H/R injury and was reversed to near-normal levels with Mst1 deletion via inhibiting the GSK3β-p53 axis (Fig. 8B). Regarding mitochondrial function, the opening rate of the mitochondrial permeability transition pore (mPTP) was increased in H/R-treated cells and was reduced in response to Mst1 deletion or SB216763 (Fig. 8C). Similarly, mitochondria ATP production was repressed in H/R-treated cells and was reversed to near-normal levels with Mst1 deletion via regulating the GSK3β-p53 axis (Fig. 8D). Regarding mitochondrial apoptosis, caspase-9 activity was measured. H/R-mediated caspase-9 activation was reversed by Mst1 deletion, similar to the results obtained with treatment with SB21673 (Fig. 8E). Altogether, our data indicate that the GSK3β-p53 axis is also involved in H/R-mediated renal tubular epithelial cell apoptosis and mitochondrial damage.

4. Discussion

Renal I/R injury, a leading cause of AKI, accounts for the acute drop in renal function and is the independent risk factor for the development of chronic kidney disease [38]. Kidneys subjected to I/R injury are primarily characterized by the death of renal tubular epithelial cells due to poorly understood mechanisms [39]. In the present study, we found that Mst1 could be considered the primary pathogenesis for renal I/R injury. Our data demonstrated that Mst1 was drastically upregulated after renal I/R injury, and higher Mst1 expression was closely associated with renal dysfunction, an excessive inflammatory reaction, uncontrolled oxidative stress, and extensive renal tubular epithelial cell apoptosis. However, genetic ablation of Mst1 reversed renal function and protected the kidney against I/R injury. Functional assays

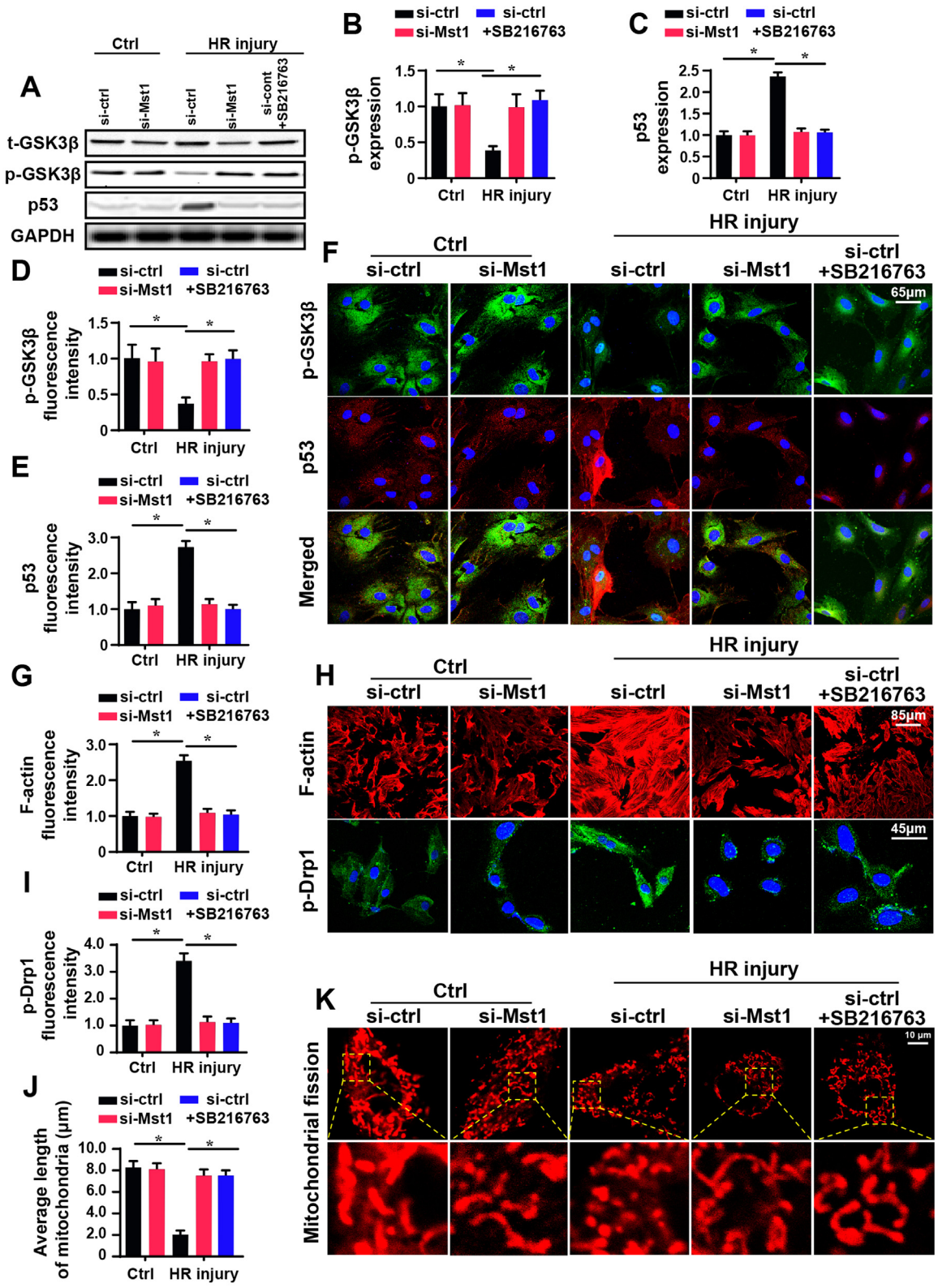

Fig. 7. Mst1 regulates Drp1 phosphorylation and F-actin accumulation via GSK3β-p53 signalling pathway. A-C. In vitro, the renal tubular epithelial cell line LLC-PK1 was used with a hypoxia and reoxygenation (H/R) stimulus to mimic animal I/R injury. siRNA against Mst1 and control siRNA were transfected into cell in vitro. SB216763 was used to inhibit GSK3β activity. The signalling pathway of GSK3β-p53 axis was determined via western blotting. **D-F.** Immunofluorescence assay for GSK3β and p53 in response to H/R injury and Mst1 deletion. **G-I.** After inhibition of GSK3β, the Drp1 phosphorylation at Ser616 and F-actin polymerization were measured via immunofluorescence. Mst1 deletion repressed F-actin accumulation and Drp1 phosphorylation, similar to the results obtained via inhibiting GSK3β-p53 signalling pathway. **J-K.** Mitochondrial fission was observed using immunofluorescence. SB216763 was used to inhibit GSK3β activity. *P < 0.05.

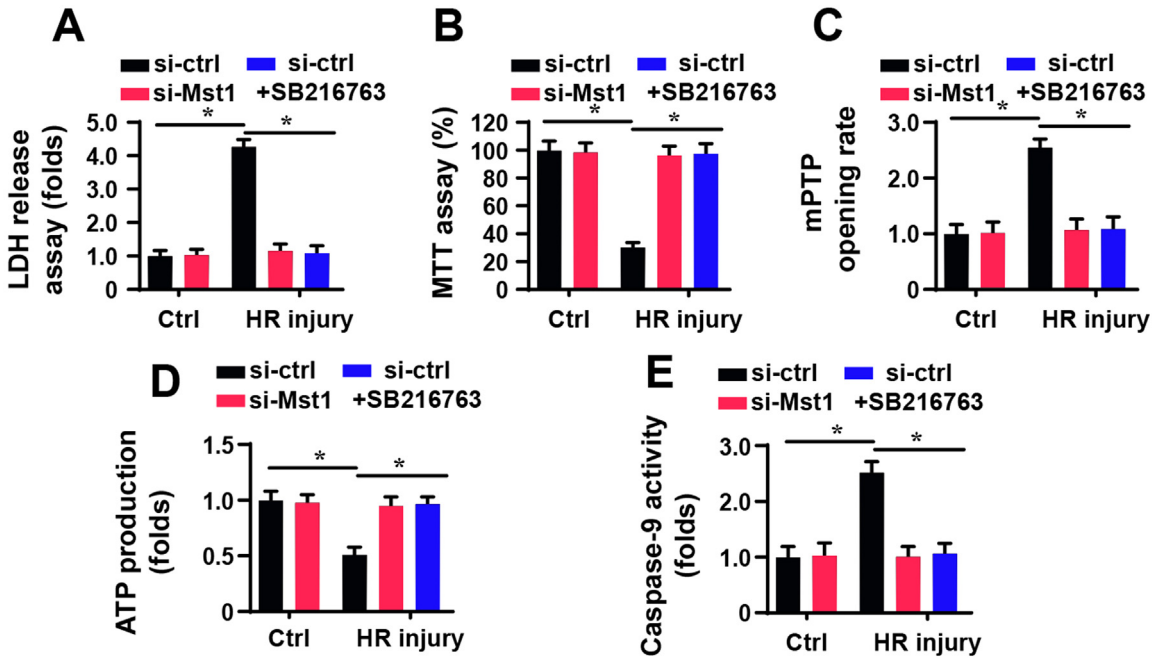

Fig. 8. GSK3β-p53 signalling pathway is also involved in mitochondrial dysfunction and renal tubular epithelial cell apoptosis. A. In vitro, the renal tubular epithelial cell line LLC-PK1 was used with a hypoxia and reoxygenation (H/R) stimulus to mimic animal I/R injury. siRNA against Mst1 and control siRNA were transfected into cell in vitro. SB216763 was used to inhibit GSK3β activity. LDH release assay was performed to analyse the cell death. **B.** MTT assay for cell viability. **C.** To verify the role of GSK3β-p53 signalling pathway in mitochondrial damage, mPTP opening was determined. **D.** ATP production was evaluated via ELISA. **E.** Caspase-9 activity was estimated to reflect the mitochondrial apoptosis. *P < 0.05.

demonstrated that Mst1 upregulation was associated with GSK3β-p53 axis activation, and the latter induced mitochondrial fission via two mechanisms. One was driven by Drp1 phosphorylation at Ser616, and the other involved the induction of F-actin polymerization. With the help of Drp1 phosphorylation and F-actin assembly, mitochondrial fission was activated and contributed to the mitochondrial potential reduction, ROS overproduction, mPTP opening and, cyt-c liberation, finally leading to the initiation of caspase-9-related mitochondrial apoptosis. This finding helps us to lay the foundation to deeply understand the aetiology of renal I/R injury and defines Mst1 as the pathogenic factor involved in acute kidney reperfusion stress via modulation of mitochondrial fission and the GSK3β-p53 axis.

The mitochondrial mass is rich in kidney cells. Additionally, the kidney has high mitochondrial oxidative metabolism and is exquisitely sensitive to hypoxic injury [40,41]. The function of renal tubular epithelial cells is primarily modulated by mitochondrial metabolism, making them more vulnerability to mitochondrial damage [42]. Accumulative evidence has established the critical role of mitochondrial injury in renal I/R injury. For example, elevated mitochondrial oxidative stress and deteriorated mitochondrial enzyme activation have been noted in the reperfused kidney [43]. In addition, inhibition of mitochondrial permeability transition pore opening via CsA has been proven to be beneficial for kidneys in the context of I/R injury [44]. Moreover, mitochondrial apoptosis has been acknowledged as the primary reason for reperfusion-mediated renal tubular epithelial cell apoptosis [45]. In addition, mitochondrial DNA damage [46], mitochondrial biosynthesis disorder [47], and mitophagy delay [48] have been found to be implicated in mitochondrial dysfunction and renal damage exerted by I/R injury. In the present study, we also found that mitochondria were the potential target of the renal I/R injury. Mitochondrial damage, such as mitochondrial potential reduction, ROS overproduction, energy undersupply, pro-apoptotic factor leakage, and caspase-9 activation, was fine-tuned by I/R injury. In addition, we illustrated that mitochondrial damage was attributable to mitochondrial fission. Inhibition of mitochondrial fission blocked caspase-3 activation and attenuated reperfusion-mediated death in renal tubular epithelial cells. This finding is similar to that in previous reports demonstrating that mitochondrial fission is harmful for the reperfused kidney [49,50]. Therefore, this evidence firmly establishes the central role of mitochondria and the subsequent mitochondrial damage that amplifies the damage signal for the reperfused kidney.

Despite the extensive research carried out over the past decades to determine the molecular features of mitochondrial fission in renal I/R injury, the upstream regulators of mitochondrial fission activation are poorly understood. In the present study, we confirm that Mst1 is the initial signal for mitochondrial fission execution. Mst1, the downstream effector of the Hippo signalling pathway, is originally identified as the apoptotic trigger in several diseases such as post-infarction cardiac remodelling [51], breast cancer [52], acute brain injury [53] and liver fibrosis [54]. Notably, the action of Mst1 in kidney damage has not yet been explained. Accordingly, this is the first detailed investigation to uncover the causal relationship between Mst1 activation and acute renal damage. Our study demonstrates that renal I/R injury augments Mst1 expression, which causes a loss of mitochondrial function and renal tubular epithelial cell apoptosis via modulation of mitochondrial fission. The mechanisms by which Mst1 modifies mitochondrial fission are attributed to Drp1 phosphorylation and F-actin polymerization. First, Drp1 phosphorylation promotes its translocation from the cytoplasm to the surface of the mitochondria where Drp1 forms the contractive ring around the mitochondria [55]. Second, F-actin polymerization empowers circular Drp1 to complete the contraction [56,57], forcing the mitochondria divide into fragments. Although Drp1 modification and F-actin stabilization have been extensively proven to be involved in mitochondrial fission, no study is available to explain whether Mst1 can modulate both Drp1 and F-actin. Our finding helps to fill this gap. Additionally, our study confirms that Mst1 modulates Drp1 phosphorylation and F-actin homeostasis via the GSK3β-p53 axis. Previous studies have noted the key role played by the GSK3β-p53 cascade in aggravating heart, liver and renal I/R injury [58]. In addition, several studies have indicated the regulatory effects of the GSK3β-p53

signalling pathway on mitochondrial fission in many acute and/or chronic diseases, including fatty liver disease, neuronal I/R injury [56], myocardial I/R injury [59], Alzheimer's disease [60], and cancer [61]. In the present study, we demonstrate that the GSK3β-p53 signalling pathway is regulated by Mst1 in the setting of renal I/R injury for the first time. Our conclusion highlights the mechanism controlling the GSK3β-p53 axis in acute kidney reperfusion injury and the relevance of GSK3β-p53 signalling in the management of mitochondrial fission.

Collectively, our results investigated the pathogenesis of renal I/R injury and showed that Mst1-mediated mitochondrial fission via Drp1 phosphorylation, F-actin assembly, and the GSK3β-p53 signalling pathway was associated with reperfusion-mediated renal malfunction and tubular epithelial cell apoptosis. This finding may pave the way to new treatment modalities, which are needed for the treatment of renal I/R injury.

Conflict of interest statement

The authors declared that they have no conflicts of interest.

References

[1] H. Nishikawa, Y. Taniguchi, T. Matsumoto, N. Arima, M. Masaki, Y. Shimamura, K. Inoue, T. Horino, S. Fujimoto, K. Ohko, T. Komatsu, K. Udaka, S. Sano, Y. Terada, Knockout of the interleukin-36 receptor protects against renal ischemia-reperfusion injury by reduction of proinflammatory cytokines, Kidney Int. 93 (3) (2018) 599–614.

[2] R. Micanovic, S. Khan, D. Janosevic, M.E. Lee, T. Hato, E.F. Srour, S. Winfree, J. Ghosh, Y. Tong, S.E. Rice, P.C. Dagher, X.R. Wu, T.M. El-Achkar, Tamm-Horsfall protein regulates mononuclear phagocytes in the kidney, J. Am. Soc. Nephrol. 29 (3) (2018) 841–856.

[3] F. Liu, W. Ni, J. Zhang, G. Wang, F. Li, W. Ren, Administration of curcumin protects kidney tubules against renal ischemia-reperfusion injury (RIRI) by odulating ntric oxide (NO) signaling pathway, Cell Physiol. Biochem. 44 (1) (2017) 401–411.

[4] L. Wei, X. Zhang, Q. Ye, Y. Yang, X. Chen, The transfection of A20 gene prevents kidney from ischemia reperfusion injury in rats, Mol. Med. Rep. 16 (2) (2017) 1486–1492.

[5] H. Zhou, P. Zhu, J. Wang, H. Zhu, J. Ren, Y. Chen, Pathogenesis of cardiac ischemia reperfusion injury is associated with CK2alpha-disturbed mitochondrial homeostasis via suppression of FUNDC1-related mitophagy, Cell Death Differ. 25 (6) (2018) 1080–1093.

[6] H. Zhou, J. Wang, P. Zhu, S. Hu, J. Ren, Ripk3 regulates cardiac microvascular reperfusion injury: the role of IP3R-dependent calcium overload, XO-mediated oxidative stress and F-action/filopodia-based cellular migration, Cell Signal 45 (2018) 12–22.

[7] H. Zhou, C. Shi, S. Hu, H. Zhu, J. Ren, Y. Chen, BI1 is associated with microvascular protection in cardiac ischemia reperfusion injury via repressing Syk-Nox2-Drp1-mitochondrial fission pathways, Angiogenesis 21 (3) (2018) 599–615.

[8] H. Zhou, J. Wang, P. Zhu, H. Zhu, S. Toan, S. Hu, J. Ren, Y. Chen, NR4A1 aggravates the cardiac microvascular ischemia reperfusion injury through suppressing FUNDC1-mediated mitophagy and promoting Mff-required mitochondrial fission by CK2alpha, Basic Res. Cardiol. 113 (4) (2018) 23.

[9] H. Zhu, Q. Jin, Y. Li, Q. Ma, J. Wang, D. Li, H. Zhou, Y. Chen, Melatonin protected cardiac microvascular endothelial cells against oxidative stress injury via suppression of IP3R-[Ca(2+)]c/VDAC-[Ca(2+)]m axis by activation of MAPK/ERK signaling pathway, Cell Stress Chaperon-. 23 (1) (2018) 101–113.

[10] P. Zhu, S. Hu, Q. Jin, D. Li, F. Tian, S. Toan, Y. Li, H. Zhou, Y. Chen, Ripk3 promotes ER stress-induced necroptosis in cardiac IR injury: a mechanism involving calcium overload/XO/ROS/mPTP pathway, Redox Biol. 16 (2018) 157–168.

[11] H. Zhou, D. Li, P. Zhu, Q. Ma, S. Toan, J. Wang, S. Hu, Y. Chen, Y. Zhang, Inhibitory effect of melatonin on necroptosis via repressing the Ripk3-PGAM5-CypD-mPTP pathway attenuates cardiac microvascular ischemia-reperfusion injury, J. Pineal Res. (2018) e12503.

[12] Q. Jin, R. Li, N. Hu, T. Xin, P. Zhu, S. Hu, S. Ma, H. Zhu, J. Ren, H. Zhou, DUSP1 alleviates cardiac ischemia/reperfusion injury by suppressing the Mff-required mitochondrial fission and Bnip3-related mitophagy via the JNK pathways, Redox Biol. 14 (2018) 576–587.

[13] H. Zhou, P. Zhu, J. Guo, N. Hu, S. Wang, D. Li, S. Hu, J. Ren, F. Cao, Y. Chen, Ripk3 induces mitochondrial apoptosis via inhibition of FUNDC1 mitophagy in cardiac IR injury, Redox Biol. 13 (2017) 498–507.

[14] H. Zhou, Y. Zhang, S. Hu, C. Shi, P. Zhu, Q. Ma, Q. Jin, F. Cao, F. Tian, Y. Chen, Melatonin protects cardiac microvasculature against ischemia/reperfusion injury via suppression of mitochondrial fission-VDAC1-HK2-mPTP-mitophagy axis, J. Pineal Res. 63 (1) (2017).

[15] D.C. Fuhrmann, B. Brune, Mitochondrial composition and function under the control of hypoxia, Redox Biol. 12 (2017) 208–215.

[16] H. Zhou, S. Wang, P. Zhu, S. Hu, Y. Chen, J. Ren, Empagliflozin rescues diabetic myocardial microvascular injury via AMPK-mediated inhibition of mitochondrial fission, Redox Biol. 15 (2018) 335–346.

[17] H. Zhou, S. Hu, Q. Jin, C. Shi, Y. Zhang, P. Zhu, Q. Ma, F. Tian, Y. Chen, Mff-dependent mitochondrial fission contributes to the pathogenesis of cardiac microvasculature ischemia/reperfusion Injury via induction of mROS-mediated cardiolipin oxidation and HK2/VDAC1 disassociation-involved mPTP opening, J. Am. Heart Assoc. 6 (3) (2017).

[18] N.J.R. Blackburn, B. Vulesevic, B. Mcneill, C.E. Cimenci, A. Ahmadi, M. Gonzalez-Gomez, A. Ostojic, Z. Zhong, M. Brownlee, P.J. Beisswenger, R.W. Milne, E.J. Suuronen, Methylglyoxal-derived advanced glycation end products contribute to negative cardiac remodeling and dysfunction post-myocardial infarction, Basic Res. Cardiol. 112 (5) (2017) 57.

[19] C. Shi, Y. Cai, Y. Li, Y. Li, N. Hu, S. Ma, S. Hu, P. Zhu, W. Wang, H. Zhou, Yap promotes hepatocellular carcinoma metastasis and mobilization via governing cofilin/F-actin/lamellipodium axis by regulation of JNK/Bnip3/SERCA/CaMKII pathways, Redox Biol. 14 (2018) 59–71.

[20] Q. Zhao, M. Ye, W. Yang, M. Wang, M. Li, C. Gu, L. Zhao, Z. Zhang, W. Han, W. Fan, Y. Meng, Effect of Mst1 on endometriosis apoptosis and migration: role of Drp1-related mitochondrial fission and Parkin-required mitophagy, Cell Physiol. Biochem. 45 (3) (2018) 1172–1190.

[21] S.H. Chang, Y.H. Yeh, J.L. Lee, Y.J. Hsu, C.T. Kuo, W.J. Chen, Transforming growth factor-beta-mediated CD44/STAT3 signaling contributes to the development of atrial fibrosis and fibrillation, Basic Res. Cardiol. 112 (5) (2017) 58.

[22] M. Ackermann, Y.O. Kim, W.L. Wagner, D. Schuppan, C.D. Valenzuela, S.J. Mentzer, S. Kreuz, D. Stiller, L. Wollin, M.A. Konerding, Effects of nintedanib on the microvascular architecture in a lung fibrosis model, Angiogenesis 20 (3) (2017) 359–372.

[23] S. Yu, X. Wang, P. Geng, X. Tang, L. Xiang, X. Lu, J. Li, Z. Ruan, J. Chen, G. Xie, Z. Wang, J. Ou, Y. Peng, X. Luo, X. Zhang, Y. Dong, X. Pang, H. Miao, H. Chen, H. Liang, Melatonin regulates PARP1 to control the senescence-associated secretory phenotype (SASP) in human fetal lung fibroblast cells, J. Pineal Res. 63 (1) (2017).

[24] X. Rossello, D.M. Yellon, The risk pathway and beyond, Basic Res. Cardiol. 113 (1) (2017) 2.

[25] T.D. Nauta, M. Van Den Broek, S. Gibbs, T.C. Van Der Pouw-Kraan, C.B. Oudejans, V.W. Van Hinsbergh, P. Koolwijk, Identification of HIF-2alpha-regulated genes that play a role in human microvascular endothelial sprouting during prolonged hypoxia in vitro, Angiogenesis 20 (1) (2017) 39–54.

[26] V. Jahandiez, M. Cour, T. Bochaton, M. Abrial, J. Loufouat, A. Gharib, A. Varennes, M. Ovize, L. Argaud, Fast therapeutic hypothermia prevents post-cardiac arrest syndrome through cyclophilin D-mediated mitochondrial permeability transition inhibition, Basic Res. Cardiol. 112 (4) (2017) 35.

[27] E. Nunez-Gomez, M. Pericacho, C. Ollauri-Ibanez, C. Bernabeu, J.M. Lopez-Novoa, The role of endoglin in post-ischemic revascularization, Angiogenesis 20 (1) (2017) 1–24.

[28] K. Wang, T.Y. Gan, N. Li, C.Y. Liu, L.Y. Zhou, J.N. Gao, C. Chen, K.W. Yan, M. Ponnusamy, Y.H. Zhang, P.F. Li, Circular RNA mediates cardiomyocyte death via miRNA-dependent upregulation of MTP18 expression, Cell Death Differ. 24 (6) (2017) 1111–1120.

[29] Y. Zhang, H. Zhou, W. Wu, C. Shi, S. Hu, T. Yin, Q. Ma, T. Han, Y. Zhang, F. Tian, Y. Chen, Liraglutide protects cardiac microvascular endothelial cells against hypoxia/reoxygenation injury through the suppression of the SR-Ca(2+)-XO-ROS axis via activation of the GLP-1R/PI3K/Akt/survivin pathways, Free Radic. Biol. Med. 95 (2016) 278–292.

[30] W. Zhang, A. Tao, T. Lan, G. Cepinskas, R. Kao, C.M. Martin, T. Rui, Carbon monoxide releasing molecule-3 improves myocardial function in mice with sepsis by inhibiting NLRP3 inflammasome activation in cardiac fibroblasts, Basic Res. Cardiol. 112 (2) (2017) 16.

[31] V. Torres-Estay, D.V. Carreno, P. Fuenzalida, A. Watts, I.F. San Francisco, V.P. Montecinos, P.C. Sotomayor, J. Ebos, G.J. Smith, A.S. Godoy, Androgens modulate male-derived endothelial cell homeostasis using androgen receptor-dependent and receptor-independent mechanisms, Angiogenesis 20 (1) (2017) 25–38.

[32] C. Zong, D. Qin, C. Yu, P. Gao, J. Chen, S. Lu, Y. Zhang, Y. Liu, Y. Yang, Z. Pu, X. Li, Y. Fu, Q. Guan, X. Wang, The stress-response molecule NR4A1 resists ROS-induced pancreatic beta-cells apoptosis via WT1, Cell Signal. 35 (2017) 129–139.

[33] R. Zhang, Y. Sun, Z. Liu, W. Jin, Y. Sun, Effects of melatonin on seedling growth, mineral nutrition, and nitrogen metabolism in cucumber under nitrate stress, J. Pineal Res. 62 (4) (2017).

[34] P.T. Kang, C.L. Chen, P. Lin, W.M. Chilian, Y.R. Chen, Impairment of pH gradient and membrane potential mediates redox dysfunction in the mitochondria of the post-ischemic heart, Basic Res. Cardiol. 112 (4) (2017) 36.

[35] H. Zhou, Q. Ma, P. Zhu, J. Ren, R.J. Reiter, Y. Chen, Protective role of melatonin in cardiac ischemia-reperfusion injury: from pathogenesis to targeted therapy, J. Pineal Res. 64 (3) (2018).

[36] R. Li, T. Xin, D. Li, C. Wang, H. Zhu, H. Zhou, Therapeutic effect of Sirtuin 3 on ameliorating nonalcoholic fatty liver disease: the role of the ERK-CREB pathway and Bnip3-mediated mitophagy, Redox Biol. 18 (2018) 229–243.

[37] H. Zhou, S. Wang, S. Hu, Y. Chen, J. Ren, ER-mitochondria microdomains in cardiac ischemia-reperfusion ijury: a fresh perspective, Front. Physiol. 9 (2018) 755.

[38] J.R. Kingery, T. Hamid, R.K. Lewis, M.A. Ismahil, S.S. Bansal, G. Rokosh, T.M. Townes, S.T. Ildstad, S.P. Jones, S.D. Prabhu, Leukocyte iNOS is required for inflammation and pathological remodeling in ischemic heart failure, Basic Res. Cardiol. 112 (2) (2017) 19.

[39] M. Merjaneh, A. Langlois, S. Larochelle, C.B. Cloutier, S. Ricard-Blum, V.J. Moulin, Pro-angiogenic capacities of microvesicles produced by skin wound myofibroblasts, Angiogenesis 20 (3) (2017) 385–398.

[40] M. Rienks, P. Carai, N. Bitsch, M. Schellings, M. Vanhaverbeke, J. Verjans, I. Cuijpers, S. Heymans, A. Papageorgiou, Sema3A promotes the resolution of cardiac inflammation after myocardial infarction, Basic Res. Cardiol. 112 (4)

(2017) 42.
[41] S. Lin, K. Hoffmann, C. Gao, M. Petrulionis, I. Herr, P. Schemmer, Melatonin promotes sorafenib-induced apoptosis through synergistic activation of JNK/c-jun pathway in human hepatocellular carcinoma, J. Pineal Res. 62 (3) (2017).
[42] H.J. Lee, Y.H. Jung, G.E. Choi, S.H. Ko, S.J. Lee, S.H. Lee, H.J. Han, BNIP3 induction by hypoxia stimulates FASN-dependent free fatty acid production enhancing therapeutic potential of umbilical cord blood-derived human mesenchymal stem cells, Redox Biol. 13 (2017) 426–443.
[43] D. Shin, E.H. Kim, J. Lee, J.L. Roh, RITA plus 3-MA overcomes chemoresistance of head and neck cancer cells via dual inhibition of autophagy and antioxidant systems, Redox Biol. 13 (2017) 219–227.
[44] M. Tomczyk, I. Kraszewska, K. Szade, K. Bukowska-Strakova, M. Meloni, A. Jozkowicz, J. Dulak, A. Jazwa, Splenic Ly6C(hi) monocytes contribute to adverse late post-ischemic left ventricular remodeling in heme oxygenase-1 deficient mice, Basic Res. Cardiol. 112 (4) (2017) 39.
[45] C. Sarkar, R.K. Ganju, V.J. Pompili, D. Chakroborty, Enhanced peripheral dopamine impairs post-ischemic healing by suppressing angiotensin receptor type 1 expression in endothelial cells and inhibiting angiogenesis, Angiogenesis 20 (1) (2017) 97–107.
[46] H.Y. Lee, K. Back, Melatonin is required for H2 O2 - and NO-mediated defense signaling through MAPKKK3 and OXI1 in Arabidopsis thaliana, J. Pineal Res. 62 (2) (2017).
[47] L. Xiao, X. Xu, F. Zhang, M. Wang, Y. Xu, D. Tang, J. Wang, Y. Qin, Y. Liu, C. Tang, L. He, A. Greka, Z. Zhou, F. Liu, Z. Dong, L. Sun, The mitochondria-targeted antioxidant MitoQ ameliorated tubular injury mediated by mitophagy in diabetic kidney disease via Nrf2/PINK1, Redox Biol. 11 (2017) 297–311.
[48] L.A. Vargas, F.C. Velasquez, B.V. Alvarez, Compensatory role of the NBCn1 sodium/bicarbonate cotransporter on Ca(2+)-induced mitochondrial swelling in hypertrophic hearts, Basic Res. Cardiol. 112 (2) (2017) 14.
[49] Z. Hu, J. Cheng, J. Xu, W. Ruf, C.J. Lockwood, Tissue factor is an angiogenic-specific receptor for factor VII-targeted immunotherapy and photodynamic therapy, Angiogenesis 20 (1) (2017) 85–96.
[50] W.R. Garcia-Nino, F. Correa, J.I. Rodriguez-Barrena, J.C. Leon-Contreras, M. Buelna-Chontal, E. Soria-Castro, R. Hernandez-Pando, J. Pedraza-Chaverri, C. Zazueta, Cardioprotective kinase signaling to subsarcolemmal and interfibrillar mitochondria is mediated by caveolar structures, Basic Res. Cardiol. 112 (2) (2017) 15.
[51] J.M. Pickard, N. Burke, S.M. Davidson, D.M. Yellon, Intrinsic cardiac ganglia and acetylcholine are important in the mechanism of ischaemic preconditioning, Basic Res. Cardiol. 112 (2) (2017) 11.
[52] R. Jokinen, S. Pirnes-Karhu, K.H. Pietilainen, E. Pirinen, Adipose tissue NAD (+)-homeostasis, sirtuins and poly(ADP-ribose) polymerases -important players in mitochondrial metabolism and metabolic health, Redox Biol. 12 (2017) 246–263.
[53] L. Han, H. Wang, L. Li, X. Li, J. Ge, R.J. Reiter, Q. Wang, Melatonin protects against maternal obesity-associated oxidative stress and meiotic defects in oocytes via the SIRT3-SOD2-dependent pathway, J. Pineal Res. 63 (3) (2017).
[54] N. Jovancevic, A. Dendorfer, M. Matzkies, M. Kovarova, J.C. Heckmann, M. Osterloh, M. Boehm, L. Weber, F. Nguemo, J. Semmler, J. Hescheler, H. Milting, E. Schleicher, L. Gelis, H. Hatt, Medium-chain fatty acids modulate myocardial function via a cardiac odorant receptor, Basic Res. Cardiol. 112 (2) (2017) 13.
[55] T. Fan, H. Pi, M. Li, Z. Ren, Z. He, F. Zhu, L. Tian, M. Tu, J. Xie, M. Liu, Y. Li, M. Tan, G. Li, W. Qing, R.J. Reiter, Z. Yu, H. Wu, Z. Zhou, Inhibiting MT2-TFE3-dependent autophagy enhances melatonin-induced apoptosis in tongue squamous cell carcinoma, J. Pineal Res. 64 (2) (2018).
[56] C. Ronchi, E. Torre, R. Rizzetto, J. Bernardi, M. Rocchetti, A. Zaza, Late sodium current and intracellular ionic homeostasis in acute ischemia, Basic Res. Cardiol. 112 (2) (2017) 12.
[57] D. Feng, B. Wang, L. Wang, N. Abraham, K. Tao, L. Huang, W. Shi, Y. Dong, Y. Qu, Pre-ischemia melatonin treatment alleviated acute neuronal injury after ischemic stroke by inhibiting endoplasmic reticulum stress-dependent autophagy via PERK and IRE1 signalings, J. Pineal Res. 62 (3) (2017).
[58] X. Shen, B. Hu, G. Xu, F. Chen, R. Ma, N. Zhang, J. Liu, X. Ma, J. Zhu, Y. Wu, R. Shen, Activation of Nrf2/HO-1 pathway by glycogen synthase kinase-3beta inhibition attenuates renal ischemia/reperfusion injury in diabetic rats, Kidney Blood Press Res. 42 (2) (2017) 369–378.
[59] K. Lee, K. Back, Overexpression of rice serotonin N-acetyltransferase 1 in transgenic rice plants confers resistance to cadmium and senescence and increases grain yield, J. Pineal Res. 62 (3) (2017).
[60] T.D. Le Cras, P.S. Mobberley-Schuman, M. Broering, L. Fei, C.C. Trenor 3rd, D.M. Adams, Angiopoietins as serum biomarkers for lymphatic anomalies, Angiogenesis 20 (1) (2017) 163–173.
[61] V. Randriamboavonjy, A. Kyselova, A. Elgheznawy, S. Zukunft, I. Wittig, I. Fleming, Calpain 1 cleaves and inactivates prostacyclin synthase in mesenteric arteries from diabetic mice, Basic Res. Cardiol. 112 (1) (2017) 10.